Published in final edited form as:
Clin Cancer Res. 2011 May 15; 17(10): 3112–3122. doi:10.1158/1078-0432.CCR-10-1264.

Fyn is downstream of the HGF/MET signaling axis and affects cellular shape and tropism in PC3 cells

Ana R. Jensen[1,*], **Y. David Saito**[1,*], **Chuanhong Liao**[3], **Jinlu Dai**[4], **Evan T. Keller**[4], **Hikmat Al-Ahmadie**[5], **Kelly Dakin Haché**[6], **Peter Usatyuk**[7], **Margarit Sievert**[1], **Gladell P. Paner**[8], **Soheil Yala**[1], **Gustavo M. Cervantes**[1], **Viswanathan Natarajan**[7], **Ravi Salgia**[1], and **Edwin M. Posadas**[1,2,9]

[1] Section of Hematology/Oncology, Department of Medicine, University of Chicago

[2] Section of Urology, Department of Surgery, University of Chicago

[3] Biostatistics Core, Department of Heath Studies, University of Chicago

[4] Department of Urology, University of Michigan School of Medicine

[5] Department of Pathology, Memorial Sloan-Kettering Cancer Center

[6] Department of Pathology and Laboratory Medicine, Dalhousie University

[7] Department of Pharmacology, University of Illinois at Chicago

[8] Department of Pathology, University of Chicago

[9] Division of Hematology/Oncology, Department of Medicine and Samuel Ochin Comprehensive Cancer Institute, Cedars-Sinai Medical Center

Abstract

Purpose—Fyn is a member of the Src family of kinases that we have previously shown to be overexpressed in prostate cancer. This study defines the biological impact of Fyn inhibition in cancer using a PC3 prostate cancer model.

Experimental Design—Fyn expression was suppressed in PC3 cells using an shRNA against Fyn (PC3/FYN-). Knockdown cells were characterized using standard growth curves and time-lapse video microscopy of wound assays and Dunn Chamber assays. Tissue microarray analysis was used to verify the physiologic relevance of the HGF/MET axis in human samples. Flank injections of nude mice were performed to assess *in vivo* growth characteristics.

Results—HGF was found to be sufficient to drive Fyn mediated events. Compared to control transductants (PC3/Ctrl), PC3/FYN- showed a 21% decrease in growth at 4 days (P=0.05). PC3/FYN- cells were 34% longer than control cells (P=0.018) with 50% increase in overall surface area (P<0.001). Furthermore, when placed in a gradient of HGF, PC3/FYN- cells showed impaired directed chemotaxis down an HGF gradient in comparison to PC3/Ctrl (P=0.001) despite a 41% increase in cellular movement speed. *In vivo* studies showed 66% difference of PC3/FYN- cell growth at 8 weeks using bidimensional measurements (P=0.002).

Conclusions—Fyn plays an important role in prostate cancer biology by facilitating cellular growth and by regulating directed chemotaxis- a key component of metastasis. This finding bears particular translational importance when studying the effect of Fyn inhibition in human subjects.

Corresponding Author: Edwin M. Posadas, M.D., 8700 Beverly Blvd, Cancer Institute North Tower, Mezzanine Level C2002, Los Angeles, CA 90048, eposadas@bsd.uchicago.edu.
*Authors contributed equally to this work and share lead authorship

Keywords

Fyn; prostate cancer; cell shape; cell motility; HGF

Introduction

The Src-family kinases (SFKs) have long been recognized as key players in cancer biology. Currently, the known members of the SFKs include Src, Lck, Fyn, Yes, Fgr, Lyn, Hck, Blk, and Yrk, and all these family members share a common structure and pattern of activation. The existence of a unique domain provides high variability and impacts protein-protein interactions that confer specific physiologic and pathophysiologic function for each member.

Fyn is a ubiquitously expressed SFK that has been previously demonstrated by our group to be overexpressed in prostate cancer (1). Fyn is localized to the inner cytoplasmic leaflet of plasma membrane; a process is driven by post-translational fatty acid acylation of amino acids in the SH4-domain, typically with myristatic- and palmitatic-acids, as well as methylation of lysine residues (2, 3). Activation of Fyn results in tyrosine phosphorylation of a variety of target proteins resulting in downstream signaling of a number of pathways. The role of Fyn has been studied in a variety of cellular processes including T-cell and B-cell receptor signaling, oligodendrocyte, keratinocyte and natural killer cell differentiation, platelet activation, integrin and growth factor-mediated signaling, and cell-cell adhesion and cell migration (4–8). These interactions are mediated by signaling partners such as FAK and paxillin that are overexpressed in prostate cancer concurrent with Fyn (1).

Given our findings, we have made efforts to delineate the causal relationship between Fyn overexpression and prostate cancer progression. Our previous studies demonstrated a concurrent up-regulation of FAK and paxillin in prostate cancer tissues suggesting that Fyn may act as a regulator of shape and motility (1). We thus hypothesized that disruption of Fyn activity would result in impaired cellular motility and alternation of cell shape in prostate cancer. Further, up-stream of Fyn, there are a number of growth factors and receptors whose downstream signaling may be mediated by the activity of SFKs. Serum concentrations of HGF have been shown to be elevated in men with prostate cancer (9). Furthermore, MET expression has been described in several studies suggesting that this axis may be active in stimulating biochemical events related to disease progression (10); however, the role of the HGF/MET axis has not been well characterized in prostate cancer. In this study, we show that Fyn strongly impacts cellular tropism and shape and that this behavior can be driven by activation of the HGF/MET signaling axis in prostate cancer cell line.

Methods

Cells and *Fyn* knockdown

PC3 cells were a generous gift of Dr. Carrie Rinker-Schaeffer. Cells were propagated and maintained in RPMI 1640 media (Gibco BRL, Gaithersburg, MD) supplemented with 1% streptomycin/penicillin (Cellgro, Manassas, VA) and 10% fetal calf serum (Cellgro, Manassas, VA) at 37°C in humidified air at 5% CO_2, except where noted.

Suppression of *Fyn* expression was achieved using MISSION shRNA Lentiviral transduction particles (Sigma-Aldrich; St. Louis, MO). Transduction conditions were optimized with a GFP containing construct from Sigma using the same lentiviral transduction system. In the presence of hexadimethrine bromide at 8 mcg/mL, PC3 cells were transduced with shRNA against *Fyn* or a non-targeting (control) shRNA named PC3/FYN- and PC3/Ctrl, respectively. Knockdown cell lines were propagated in media

containing 0.25 mcg/mL puromycin (Sigma Chemical Co.; St. Louis, MO) as the construct contained a puromycin resistance vector. Immunoblots for Fyn were performed in conjunction with all studies to ensure continued Fyn suppression.

Antibodies

Anti-Fyn antibody for use in immunoblotting, immunohistochemistry (IHC) and immunofluorescence (IF) was purchased from Upstate Biotechnology, Inc. Rhodamine-labeled phalloidin and fluorescein isothiocyanate-conjugated anti-mouse and rhodamine-conjugated anti-rabbit antibodies for use as secondary antibodies for IF were obtained from Molecular Probes. Total MET antibody was obtained from Zymed Laboratories. Two phospho-MET antibodies were utilized for IHC (pY1003 and pY202/3/4, Biosource). HGF antibody was obtained from R&D systems.

Preparation of cell lysates and immunoblotting

Cell lysates were prepared using lysis buffer containing 20 mM Tris, pH 8.0, 150 mM NaCl, 10% glycerol, 1% Nonidet P-40, and 0.42% NaF containing inhibitors (1mM sodium orthovanadate, 1mM HALT phosphatase inhibitor cocktail (Thermo Scientific)). Cell lysates were separated using a 7.5% Tris-HCl gel with SDS-PAGE under reducing conditions. Protein was transferred to polyvinyl chloride membranes and processed for immnoblotting using established methods with enhanced chemiluminescence techniques (GE Healthcare; Buckinhamshire, UK).

Quantitative RT-PCR for FYN

RNA from cell lines was extracted using an RNAqueous kit (Ambion, Auton, TX, USA) according to the manufacturer's recommendations. Samples were stored at −80 °C until processed. Customized primers for Fyn were prepared by Integrated DNA Technologies (Coralville, IA, USA). The left primer was: 5′-ATG GAA ACA CAA AAG TAG CCA TAA A-3′; and the right primer: 5′-TCT GTG AGT AAG ATT CCA AAA GAC C-3′. Data were calibrated to the expression of glyceraldehyde phosphate dehydrogenase. Quantitative PCR was performed using SYBR Green dye on an ABI 7700 (Applied Biosystems, Foster City, CA, USA).

Time-lapse video microscopy (TLVM) and image analysis

All time-lapse experiments were performed using an inverted Olympus IX71 microscope with an attached QImaging Retiga EXi camera. Cells were maintained on a heated stage at 37°C (Omega CN9000A) with a constant flow of 5% CO_2. Image capture was achieved using IPLab version 3.65a (Scanalytics Inc). Analysis of still images was performed using the ImageJ software package from the NIH (http://rsb.info.nih.gov/ij/).

Wound-healing assay

Cells were plated onto either 60-mm plates or 6-well plates at a concentration of 1×10^6 cells/cm^2 and allowed to attach overnight. Cells were allowed to grow to approximately 80% confluence by visual inspection prior to scratch assay. At the time of the scratch, cells were washed three times with PBS and starved in serum-free RPMI 1640 for 3 hours. A linear wound was then made with a 10 μL plastic pipette tip. After washing three times with serum free media, the cells were stimulated with media containing fetal calf serum or HGF. Wound width was measured at three randomly chosen sites using ImageJ. Growth factors used included hepatocyte growth factor (HGF), epidermal growth factor (EGF), and basic fibroblast growth factor (bFGF) (Cell Signaling). Wound closure was quantified by parallel assessments of wound length at 4 fixed positions over time and expressed as a percentage of baseline wound distance at that point.

Single-cell shape and motility assay

Cells were plated onto 35-mm plates at a concentration of 1.5×10^5 cells/cm^2 and allowed to attach for 48 hours to approximately 20% confluence. The cells were then washed three times with PBS and starved for at least 3 hours. Cells were then stimulated with 10–50 ng/mL HGF and recorded as described above using TLVM. Cell movements were tracked using the Metamorph 7.6 software package (Molecular Devices). Using this software package, 15–25 cells per sample were identified and tracked over a 12 hour period. The tracking data was fed in to the IBIDI cell tracker tool in ImageJ yielding analysis of velocity and path length. Data provided represents an average the cells tracked. Shape characterizations (area, circularity, and length) were performed by manual measurements using ImageJ using no less than 20 cells. Cellular area refers to a 2-dimensional projection of the cell onto an XY plane. For membrane ruffling, cellular perimeter was manually measured to determine the fraction of total membrane perimeter involved in ruffling in ImageJ.

Dunn-chamber assay

Cell chemotaxis was studied using a Dunn chamber assay as previously described (11). In brief, a Dunn Chamber is a modified Zigmond chamber in which a diffusion gradient of a chemotactic factor was made by creating a liquid bridge across two wells: one containing media with a high concentration of a chemotactic factor and the other well containing media alone. This creates a diffusion gradient across the area where the two are connected. Glass coverslips were placed at the bottom of a 35-mm plate and to this was added 1.5×10^5 cells in RPMI supplemented with 10% FCS. Cells were allowed to attach over 24 hours then placed under serum-starved conditions with RPMI for 3 hours. The coverslip was then inverted onto a Dunn chamber (Hawksley, Lancing, UK) filled with media (no serum). The coverslip was then sealed on the outer edges with hot VALAP mixture (1:1:1 vaseline, beeswax, and paraffin). The outer chamber of the Dunn apparatus was subsequently evacuated and refilled with media supplemented with HGF at a concentration of 10 ng/mL. Cell chemotaxis was then captured by video microscopy over 3 hours. Analysis of motility was completed as described above.

Immunofluorescence

PC3 cells were plated onto a glass coverslip in a 6-well plate at a concentration of 1.5×10^5 cells/well and allowed to attach over 48 hours in media supplemented with 10% fetal calf serum. Cells were then fixed with 4% paraformaldehyde, and permeabilized with 0.1% Triton X100-PBS before blocking with 3% bovine serum albumin in TBST. The coverslips were then incubated with primary antibody in TBST at 100:1 dilution for 1 hour. Cells were subsequently washed 3× in TBST before incubating with secondary antibody and/or Rhodamine-phalloidin in TBST at 50:1 dilution for 1 hour. Cells were washed once again in TBST before mounting onto coverslips using ProLong Gold antifade mounting medium with DAPI (Invitrogen Molecular Probes). Images were analyzed using ImageJ after deconvolution using a Huygen's algorithm. Colocalization was detected using the JACOP plugin for ImageJ.

Human tissue source

All human tissue samples used in this study were obtained from the University of Chicago. Utilization of tissue was performed under an institutional review board approved protocol requiring that all samples were kept anonymous to the primary investigational team.

Tissue was analyzed in the form of 2 tissue microarrays previously fabricated by the Department of Pathology at the University of Chicago. Microarray fabrication has been

described elsewhere (12). In short, the arrays used contained specimens from 45 patients planned to have triplicate representation on the array. Each array element was 1.5 mm in diameter. Tissue samples included primary tumor from prostate cancer patients with Gleason scores of 6 to 9. When possible both normal and tumor elements were scored on a section. The identity of patients was kept blinded to the primary analytic group. A patient's sample was only considered usable if represented at least twice on the array.

Immunohistochemistry

For IHC, stained TMA sections were analyzed by a dedicated urological pathologist (H.A.A. or K.D.H.). Results were reported semi-quantitatively on a scale of 0–3 for intensity, where 0 was negative, 1 was weak, 2 was moderate and 3 was strong. The percentage of tumor staining was reported as 0–100% in increments of 10%. A composite score was formed using the product of the intensity and percentage of glands staining. Staining was performed at the following antibody concentrations: MET at 1:100, MET-Y1003 at 1:20, MET-Y1202/3/4 at 1:25, and HGF at 25μg/mL. Each TMA contained on-slide controls of lymph node tissue to ensure absence of artifacts contributing to differential staining reported.

Mice

Eight-week-old nude (nu/nu) mice (Strain code: 088, Charles River Laboratories, Wilmington, MA) were kept in a specific pathogen free colony, in microisolator cages, and were fed sterile rodent chow and sterile water *ad libitum*. All protocols were approved by the University of Michigan Animal Care and Use Committee. Tumors were harvested at necropsy and preserved in formalin. Staining was performed using standard hematoxylin and eosin (H&E) as well as CD31 (Abcam, 1:50 dilution) to asses for microvessels. H&E sections were analyzed for mitotic index (per 10 high powered field (HPF) counting up to 30 HPFs), coagulative tumor necrosis (% tumor volume), lymphoid aggregates within the tumor (per 10 HPF), ratio of epithelioid: spindled cells, and neovessel density (CD31+ with luminal formation by pathologists review).

In vivo growth assay

PC3/FYN- and PC3/Ctrl cells were harvested by trypsinization washed twice with PBS and resuspended at a density of 2×10^6 cells in100 μL PBS for each injection site. Mice were monitored for tumor growth and when detected by palpation, measurement of the tumors began. Tumor volumes were calculated by the formula: Volume =[(minimum measurement)^2 (maximum measurement)] / 2 as described by Smith (13). Tumors were measured weekly until volume exceeded 1 mm^3. Each mouse was given 2 subcutaneous doses of PC3/FYN- (right flank) and PC3/Ctrl (left flank). Alternatively, a cross product of the longest tumor diameter and one orthogonal to the longest diameter were calculated and compared. At the conclusion of the study, all mice were sacrificed, and tissue samples were collected.

Statistical analyses

All analyses were performed using SPSS version 17.0 for Windows. A general linear model (GLM) was used to compare the effects of FYN expression and HGF stimulation and their interaction on cell morphology parameters from baseline to 12 hours and to compare changes in cell length between baseline and 12 hours. To evaluate the differences of cellular shape and growth between groups (PC3/FYN- and PC3/Ctrl, serum starved and HGF stimulated), the independent-samples T test was used for the data based on specific distributional assumptions such as the normal distribution. If the data was of a non-normal distribution, then Mann-Whitney test to assess was appropriately used. The Watson-Williams test was performed for the equality of mean angle of cellular motility using

calculating angular movements from a relative origin (14). Comparisons of quantified IHC data were performed using a Wilcoxon Signed Ranks test. For *in vivo* growth studies, tumor volume and cross product data were logarithmically transformed so that a paired-samples T test could be used to assess differences of PC3/FYN- cell growth compared to PC3/Ctrl. A two-sided $p < 0.05$ was used as a threshold for declaring statistical significance.

Results

Generation of PC3 Fyn Knockdown Cell Line

To characterize the effect of Fyn variation *in vitro*, we generated a knockdown line using PC3 cells and lentiviral transduction particles containing shRNA constructs targeted specifically against *Fyn* (PC3/FYN-). Using a multiplicity of infection of 2, five constructs (Supplemental Table 1) were tested. The construct leading to maximal Fyn suppression by immunoblot with minimal effect on non-Fyn SFKs such as Src was labeled PC3/FYN- and advanced for further study. A control cell line was developed (PC3/Ctrl) using a non-targeting shRNA construct. Both lines were maintained under continuous selection of puromycin. Fyn mRNA expression was measured with a comparative RT-PCR using PC3/Ctrl as a reference and protein by immunoblot (Figure 1A,B). Both assays revealed that Fyn expression was decreased by at least 60%. Minimal off target effects were seen as evidenced by the lack of change in Src expression (Figure 1B). The knockdown effect was stable through serial passage under these conditions.

Fyn knockdown results in impaired *in vitro* growth and motility

Under standard propagation conditions, PC3/FYN- cells showed a small but statistically significant diminishment in growth rate (Figure 1C). After 4 days under standard conditions, PC3/FYN- cells grew at only 79% the rate of PC3/Ctrl cells (P=0.05).

Wound healing assays in concert with time-lapse video microscopy (TLVM) were performed to characterize motility (Figure 2A,B and Supplemental movies 1 and 2). Virtually no wound closure was seen in the absence of serum or other mitogens. However, in serum-replete conditions, PC3/Ctrl cells showed near complete closure within 12 hours whereas PC3/FYN- cells failed to show complete closure.

HGF stimulates PC3 motility

Isolated growth factors were utilized to further understand growth and motility. HGF, EGF, and bFGF were selected given overexpression or increased serum concentrations in men with advanced prostate cancer (9, 15, 16). Wound closure was observed using TLVM under conditions of media with a single growth factor at 10 ng/mL. HGF was determined to be the optimal motility stimulus for PC3 cells from this pool as it produced the highest rate of wound closure per unit time (Supplemental Figure 1).

Fyn knockdown results in altered cell shape and increased cell speed with impaired directional motility

A series of single cell motility experiments with serum or HGF stimulation were performed to measure the impact of Fyn knockdown on morphology and speed of movement.

Cell area—Area was measured as a measure of size and cell spreading. Differential effects of HGF stimulation on cell shape are summarized in Figure 3. At baseline, a small but statistically significant difference was seen between PC3/FYN- and PC3/Ctrl cells. Under serum-starved conditions, the PC3/FYN- cells were 33% larger than the PC3/Ctrl cells (P=0.018), and after 12 hours of stimulation with serum there was a 50% increase in surface

area (P<0.001) for the PC3/FYN- cells compared to PC3/Ctrl. Comparing Feret's (longest) diameter, the PC3/FYN- cells were 34% longer at baseline (P<0.001) and 56% longer after 12 hours of serum simulation (P<0.001). Membrane ruffling was not significantly different between the two cell lines before or after serum stimulation. The effect of HGF was similar on both cell lines; in comparing PC3/FYN-to PC3/Ctrl cells after 12 hours of stimulation we found a 43% increase in area (P=0.016), and 17% increase in Feret's diameter (P=0.026) with no change in ruffling.

Cell length—A similar trend was also observed for cell length as determined by longest cell axis under the same experimental conditions (Figure 3A,C). After 12 hours of stimulation with HGF, PC3/FYN- cells were 31% longer than PC3/Ctrl cells (P=0.003). In fact, PC3/Ctrl cells showed 17% increase in cell length (P=0.010) after 12 hours in HGF whereas the PC3/FYN- showed no statistically significant change.

Cell morphology—In response to HGF stimulation, PC3/FYN- acquired a broader distribution of various cell shapes and morphologies (Figure 3A,C). PC3/FYN- cells also produced a larger number of filopodia compared to PC3/Ctrl- cells. Using representative images of subconfluent cellular monolayers, we manually counted the percentage cells with filopodia. In the absence of HGF supplementation, PC3/Ctrl cells underwent a decrease of the percentage of cells with filopodia from 11% to 4.5%, a 59% decrease over 12 hours. Under the same conditions, the percentage of PC3/FYN- cells with filopodia only decreased 20%, from 40.5% to 32.5%. Under HGF stimulation, PC3/Ctrl cells had a 9% increase in cells with filopodia whereas PC3/FYN- cells had a 12% decrease over 12 hours. There were variations in the percentage of cell perimeter ruffling. PC3/Ctrl cells had a greater degree of ruffle formation in response to HGF supplementation (a 16% increase in percentage of cell circumference with ruffles upon HGF stimulation) while PC3/FYN- cells were not observed to have any change in ruffling in the presence of HGF. Cell circularity (as defined by $4\pi[\text{area}/\text{perimeter}^2]$) was calculated as an assessment of cell shape symmetry. There was an increase in circularity under serum-starved conditions over 12 hours for PC3/Ctrl cells of 12% whereas there was no significant increase observed for PC3/FYN- cells. Under HGF supplementation no changes in circularity were observed for either cell line.

To test the hypothesis that the variations in shape were related to alterations in the actin cytoskeleton, phalloidin staining with MET immunostaining were performed (Figure 3B). In response to HGF stimulation, PC3/Ctrl cells showed retraction of small hair-like projections in favor of forming larger cellular extensions. PC3/FYN- cells continued to show these small hair-like projections despite HGF stimulation.

To quantify the effect of Fyn knockdown on focal adhesion formation and MET distribution, colocalization of MET and actin was analyzed by detecting signals above a threshold level to exclude background beyond the cellular membrane- given this colocalization pattern suggests focal adhesion formation. At threshold, signal overlap between actin and MET were expressed as Mander's coefficients expressing degree over overlap. In the setting of HGF stimulation, 28% of the actin signal was associated with MET predominately at focal points along the cell surface and predominately at the tips of filopodia, which would represent focal adhesion plaque formation. Conversely, only 2% of actin was associated with HGF stimulation in PC3/FYN- cells.

Cell speed—Representative films of cellular movement of PC3/FYN- and PC3/Ctrl cells on glass bottom plates are shown in supplemental videos 3 and 4. Although PC3/FYN-cells exhibited decreased ability to migrate over monolayer defects, analysis of single cells showed a relative increase in cellular speed when no gradient was present. Both PC3/Ctrl and PC3/FYN- cells showed decreased cell speed in the absence of HGF stimulation, 24%

and 31% from baseline respectively. However, PC3/FYN- cells exhibited increased movement speed compared to PC3/Ctrl with a 41% increase in average cell speed over a 12-hour period of HGF stimulation.

Directed chemotaxis—Given the dichotomy between elevated cell speeds but decreased rates of wound closure, we hypothesized that Fyn regulates vectorial velocity or more specifically, directed chemotaxis. To test this hypothesis we employed a Dunn chamber to allow for the direct observation of cell migration under a chemotactic gradient. Unlike a Boyden Chamber assay, this allows for direct visualization of cells in transit. Individual cells were observed under TLVM for a period of 3 hours. More than 20 cells were tracked to create a composite map of movement represented as a rose plot in 10° increments (Figure 2). PC3/Ctrl cells moved toward the HGF source whereas PC3/FYN-cells were either insensitive to or moved away from the HGF source. We performed a comparison of direction relative to the vector defined by the initial and final location (Euclidean distance, ED) of the each cell (Table 1, Supplemental figure 2). In brief, this directionality coefficient is a ratio of the shortest linear distance between the ED compared to the total distance traversed by the cell (accumulated distance, AD) such that a value of 1 would represent a perfectly linear path and values below suggest relative degrees of variation from this linear path. The overall directionality did not differ greatly between the two conditions (P=0.822). However, when comparing translocation relative to the HGF source using a forward migration index (FMI) quantifying motion only in a fixed vector for each cell (i.e. a vector toward the HGF source), PC3/FYN- cells showed movement away from the gradient; PC3/Ctrl cells showed movement toward. Analysis of membrane edges revealed a greater amount of membrane ruffling in the PC3/FYN-cells relative to the PC3/Ctrl; however, comparing AD and ED, PC3/Ctrl cells were significantly more motile with and AD increase of 200% and a ED increase of 212% resulting in a 263% increase in overall vectorial velocity.

In vivo growth assay

To measure the impact specifically on growth variation in a biologically relevant system, subcutaneous flank injections were performed on 5 nude mice with each mouse receiving 2 injections of PC3/FYN- and 2 injections of PC3/Ctrl. After approximately 8 weeks of growth, mice were sacrificed and tumors measured. Four of the mice grew visible tumors. Figure 4A shows a representative mice bearing PC3/Ctrl (left or top) and PC3/FYN- (right or bottom) tumors as well as the tumors removed at necropsy. In comparing PC3/FYN- to PC3/Ctrl in each mouse (Figure 4B), an average 33% difference was seen in the size of the PC3/Ctrl and PC3/Fyn- tumors (mean volume day 43: 712 vs. 120 mm^3, P=0.014; day 57: 1299 vs. 449 mm^3; P=0.071). Alternatively, comparing the cross product of the longest diameter and an orthoganol diameter, there was a 66% difference (average cross product day 57: 570 mm2 vs 193 mm2; P=0.002). Histomorphological and immunohistochemical analysis of the tumor samples did not show significant changes in cellular morphology or tumor neovessel formation as evidenced by CD31 staining (Figure 4C). There was a trend however, to an increase in mitotic index, tumor necrosis, and tumor infiltration by lymphocytes (as evidenced by intratumoral lymphoid aggregates) favoring the PC3/Ctrl tumors without meeting significance criteria. Neovessel density was also not significantly different but favored the PC3/FYN- tumors (Figure 4D).

HGF and MET expression in prostate cancer tissue samples

The relevance of the HGF/MET signaling axis in human disease was validated by immuhistochemical analysis of a tissue microarray composed of 40 patient samples. Representative sections are shown in supplemental figure 3. HGF was upregulated 1.3-fold in cancer compared to normal (mean composite score 140.74 vs. 179.72, P=0.035). No

significant variations in MET, pMET-Y1003, or pMET-Y1349 were found in the sample population between malignant and non-malignant glands (data not shown).

Discussion

These studies show that focused reduction of Fyn expression apart from other Src-family kinases results in a notable variation in the *in vitro* phenotype. This phenotype is characterized by a change in growth kinetics that is durable over time with a significant impact upon cellular shape and motility. The *in vitro* growth studies showed a small but statistically significant separation in growth that became more pronounced during *in vivo* studies due to the significant increase in experimental duration. Further studies of multi-SFK inhibition would potentially be warranted for the future. Analysis of the tumor specimens from the mouse experiment did not show significant differences between the two conditions outside of tumor necrosis as this likely reflected the difference in size of the tumors. The lack of differences in mitotic index and neovessel formation could have been affected by tumor size and necrosis as well as loss of antigen retrieval during prolonged formalin fixation.

Our Fyn knockdown cells in general showed an accelerated speed but more importantly, aberration of directional response in PC3 cells. This change in function is accompanied by a change in macroscopic and microscopic cellular structure as shown by the variation in the arrangement of cytoskeletal elements and focal adhesions. In particular, the changes in colocalization of MET with actin points to variation in focal adhesion formation- key step in the metastatic process. This presentation is particular focused on the PC3 model given its extensive use in both *in vitro* and *in vivo* studies. Interestingly, we have found the HGF/MET axis to be a sufficient activator of Fyn-driven events. Elevation of serum HGF is well recognized in prostate cancer. Our finding of increased HGF expression in malignant prostatic glands is certainly consistent with this previous observation (9). Despite this, the expression of the MET in both total and active forms was stable to diminished. The limited sample size restricted our ability to detect more subtle differences in MET expression and activation, but if a difference was present, it would likely only represent a small variation. The role of MET in this system and in prostate cancer in general continues to be an important and exciting area of investigation that exceeds the scope of this particular study.

The SFKs are among the first oncogenes recognized in cancer biology. SFKs have remained of great interest given the central role they play in mediating extracellular stimuli to the nucleus. While the majority of research in Src biology has focused on the prototypical member of this family, c-Src, emerging data suggests that the various SFKs may affect cancer cells differently. Fyn is known to be ubiquitously expressed under normal physiologic conditions and its functions are typically ascribed to mediating T-cell response and neuronal development (17). Fyn knockout mice have been characterized as having a subtle phenotype in neuropsychological development and T-cell function with little phenotypic characteristics otherwise (18). This has been attributed to the high degree of homology of the family members that may allow for compensation for the loss or absence of another family member. There is now growing evidence, however, that non-Src SFKs play an important role in tumor progression. In a study by Park *et al*, inhibition of Lyn expression with RNAi resulted in altered cellular growth apart from migration whereas Src knockdown resulted in impaired metastatic capability (19). Similarly, our group has previously demonstrated that Fyn is upregulated in prostate cancer (1). Therefore, we have made efforts to define the role that this upregulated kinase may play in cancer biology.

Our results point toward a role for Fyn in metastatic progression, which are consistent with findings in other models (20). This finding holds particular appeal for translation in the

availability of SFK inhibitors that have entered clinical studies. It is important to note, however, that these inhibitors display varying activity on the members of the Src family and the majority of their characterization and hence development have relied upon the inhibition of Src itself. Clinical studies with such agents have shown modest benefits (21) but have been strongly dependent upon trial design. Several studies with dasatinib have been performed in prostate cancer. Araujo (22–24) has argued that the benefit of such agents may be in altering the microenvironment resulting in a cytostatic effect. A clinical trial of a potent SFK inhibitor, sacratinib (AZD0530), using PSA-driven endpoints showed no significant effect (25), but this would be less expected given the role that Fyn and other SFKs likely play in disease progression. Understanding, however, that the events related to Fyn inhibition are likely not cytotoxic and yet potent demands a more contemporary approach to experimental and clinical trial designs to test Fyn-associated hypotheses.

To optimize Fyn-targeted therapeutic approaches, however, it may be necessary to combine agents rationally to maximize effect. Thus, understanding the upstream and downstream signaling partners of Fyn becomes essential in developing new strategies. Here, we identify HGF and MET as activators of Fyn related down-stream events. Identifying and understanding interactions with downstream signaling partners such as FAK and paxillin, which we have also described as up-regulated in prostate cancer (1), may open additional therapeutic strategies that can be tested *in vivo* and in future clinical trials.

Fyn is a member of the SFKs upregulated and germane to prostate cancer progression. It functions to promote not only growth but more importantly, directed chemotaxis, a finding that makes Fyn a putative target for metastasis-directed therapy in prostate cancer and other malignancies where it is overexpressed.

Supplementary Material

Refer to Web version on PubMed Central for supplementary material.

Acknowledgments

The authors would like to thank Ms. Can Gong for her assistance in the preparation of the tissue microarrays for pathology review. Dr. Christine Labno and the University of Chicago microscopy core facility for assistance with cell tracking and immunohistochemistry analysis. We would also like to thank Dr. Karen Kaul for helping to coordinate tissue samples from the Chicago SPORE tissue bank and Ms. Leslie Martin for assistance with TMAs from the Department of Pathology at the University of Chicago. The authors would also like to express their thanks for the generous support provided by the University of Chicago Auxiliary Board, The Riviera Club, and the Arlington Million Ladies. Without their generosity, this project could not have started.

Funding sources: (EP) DOD Physician Research Training Award W81XWH-08-1-0470; Prostate SPORE Career Development Award; University of Chicago Auxiliary Board; Rivera Club; Arlington Million Ladies; (EK) P01093900; (VN) RO1 HL 079396; (RS) 5R01CA125541-04, 3R01CA125541-03S1, 5R01CA129501-02, 3R01CA129501-02S1.

References

1. Posadas EM, Al-Ahmadie H, Robinson VL, et al. FYN is overexpressed in human prostate cancer. BJU Int. 2009; 103:171–7. [PubMed: 18990162]
2. Alland L, Peseckis SM, Atherton RE, Berthiaume L, Resh MD. Dual myristylation and palmitylation of Src family member p59fyn affects subcellular localization. J Biol Chem. 1994; 269:16701–5. [PubMed: 8206991]
3. Liang X, Lu Y, Wilkes M, Neubert TA, Resh MD. The N-terminal SH4 region of the Src family kinase Fyn is modified by methylation and heterogeneous fatty acylation: role in membrane targeting, cell adhesion, and spreading. J Biol Chem. 2004; 279:8133–9. [PubMed: 14660555]

4. Calautti E, Grossi M, Mammucari C, et al. Fyn tyrosine kinase is a downstream mediator of Rho/PRK2 function in keratinocyte cell-cell adhesion. J Cell Biol. 2002; 156:137–48. [PubMed: 11777936]
5. Cary LA, Chang JF, Guan JL. Stimulation of cell migration by overexpression of focal adhesion kinase and its association with Src and Fyn. J Cell Sci. 1996; 109 (Pt 7):1787–94. [PubMed: 8832401]
6. Reddy KB, Smith DM, Plow EF. Analysis of Fyn function in hemostasis and alphaIIbbeta3-integrin signaling. J Cell Sci. 2008; 121:1641–8. [PubMed: 18430780]
7. Wolf RM, Wilkes JJ, Chao MV, Resh MD. Tyrosine phosphorylation of p190 RhoGAP by Fyn regulates oligodendrocyte differentiation. J Neurobiol. 2001; 49:62–78. [PubMed: 11536198]
8. Zamoyska R, Basson A, Filby A, Legname G, Lovatt M, Seddon B. The influence of the src-family kinases, Lck and Fyn, on T cell differentiation, survival and activation. Immunol Rev. 2003; 191:107–18. [PubMed: 12614355]
9. Humphrey PA, Zhu X, Zarnegar R, et al. Hepatocyte growth factor and its receptor (c-MET) in prostatic carcinoma. Am J Pathol. 1995; 147:386–96. [PubMed: 7639332]
10. Davies, G.; Jiang, WG.; Mason, MD. Scatter factor-hepatocyte growth factor elevation i the serum of patients with prostate cancer. In: Albin, RJ.; Mason, MD., editors. Metastasis of prostate cancer. Netherlands: Springer; 2008. p. 197-219.
11. Zicha D, Dunn G, Jones G. Analyzing chemotaxis using the Dunn direct-viewing chamber. Methods Mol Biol. 1997; 75:449–57. [PubMed: 9276291]
12. Lotan TL, Lyon M, Huo D, et al. Up-regulation of MKK4, MKK6 and MKK7 during prostate cancer progression: an important role for SAPK signalling in prostatic neoplasia. J Pathol. 2007; 212:386–94. [PubMed: 17577251]
13. Smith PC, Keller ET. Anti-interleukin-6 monoclonal antibody induces regression of human prostate cancer xenografts in nude mice. Prostate. 2001; 48:47–53. [PubMed: 11391686]
14. Zar, J. Biostatistical analysis. 5. Prentice Hall;
15. Jarrard DF, Blitz BF, Smith RC, Patai BL, Rukstalis DB. Effect of epidermal growth factor on prostate cancer cell line PC3 growth and invasion. Prostate. 1994; 24:46–53. [PubMed: 8290389]
16. Gowardhan B, Douglas DA, Mathers ME, et al. Evaluation of the fibroblast growth factor system as a potential target for therapy in human prostate cancer. Br J Cancer. 2005; 92:320–7. [PubMed: 15655558]
17. Resh MD. Fyn, a Src family tyrosine kinase. Int J Biochem Cell Biol. 1998; 30:1159–62. [PubMed: 9839441]
18. Stein PL, Lee HM, Rich S, Soriano P. pp59fyn mutant mice display differential signaling in thymocytes and peripheral T cells. Cell. 1992; 70:741–50. [PubMed: 1387588]
19. Park SI, Zhang J, Phillips KA, et al. Targeting SRC family kinases inhibits growth and lymph node metastases of prostate cancer in an orthotopic nude mouse model. Cancer Res. 2008; 68:3323–33. [PubMed: 18451159]
20. Chen ZY, Cai L, Bie P, et al. Roles of Fyn in pancreatic cancer metastasis. J Gastroenterol Hepatol. 2009
21. Yu EY, Wilding G, Posadas E, et al. Dasatinib in patients with hormone-refractory progressive prostate cancer: A phase II study. J Clin Oncol. 2008 May 20.26(suppl) abstr 5156.
22. Araujo J, Logothetis C. Dasatinib: A potent SRC inhibitor in clinical development for the treatment of solid tumors. Cancer Treat Rev. 2010
23. Araujo JC, Poblenz A, Corn P, et al. Dasatinib inhibits both osteoclast activation and prostate cancer PC-3 cell-induced osteoclast formation. Cancer Biol Ther. 2009; 8:2153–9. [PubMed: 19855158]
24. Lee YC, Huang CF, Murshed M, et al. Src family kinase/abl inhibitor dasatinib suppresses proliferation and enhances differentiation of osteoblasts. Oncogene.
25. Lara PN, Longmate J, Evans CP, et al. A phase II trial of the Src-kinase inhibitor AZD0530 in patients with advanced castration–resistant prostate cancer: a California Cancer Consortium Study. Anticancer Drugs. 2008 in press.

Statement of Translational Relevance

Fyn is a member of the SFKs that is overexpressed in prostate cancer and is potentially targetable using existing clinically usable pharmacological inhibitors. Clearly defining the Fyn phenotype is essential to developing hypotheses for clinical studies with Fyn inhibitors. This study defines such as phenotype and differs from conventional definitions of efficacy in prostate cancer by showing a distinct behavior on directional motility- a key component of metastasis. Furthermore, activation of Fyn by hepatocyte growth factor is demonstrated in laboratory samples and is relevant to human disease as shown by our immunohistochemical studies.

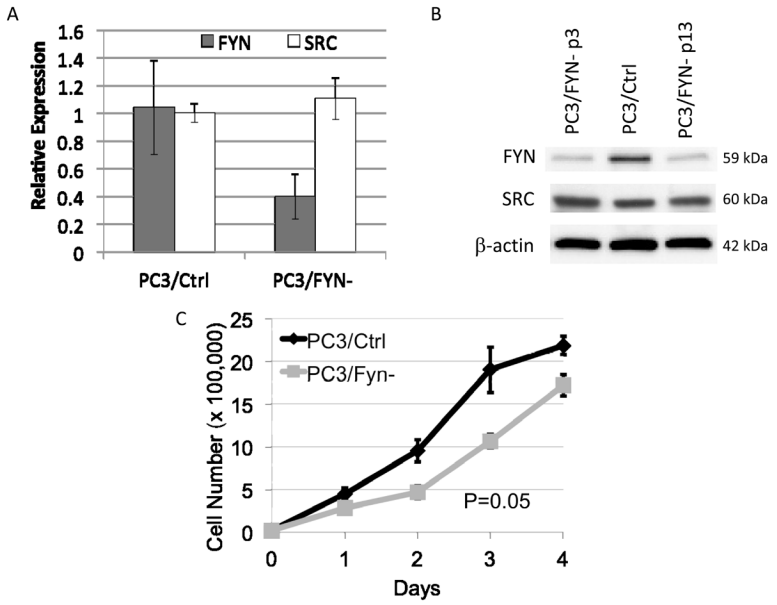

Figure 1.

Generation of Fyn knockdown cell lines (PC3/FYN-). A) Comparative RT-PCR showing mRNA expression of Fyn and Src in PC3/Ctrl and PC3/FYN- lines. Fyn expression is decreased approximately 60% without significant impact on Src expression B) Immunoblots for Fyn and Src expression showing decreased Fyn expression without significant alteration of Src expression. No significant variation in Fyn expression is seen in the PC3/FYN- line over serial passage. C) Four day growth curves comparing PC3/FYN- to PC3/Ctrl. Error bars represent standard error of the mean with 3 replicates for each day.

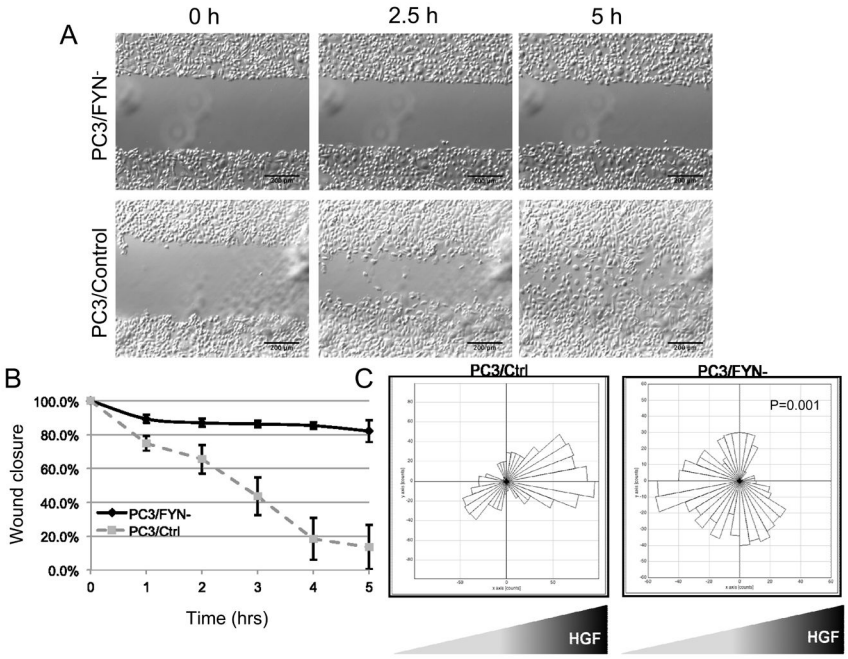

Figure 2.

Wound healing assays of PC3/FYN- and PC3/Ctrl cells in serum replete media. Full videos are available in the supplemental data. A) Representative images from time lapse video. B) Graphical representation of wound closure over time. Error bars represent standard deviation of wound closure as a percentage of the original wound distance taken at 5 serial points. C) Rose plots (circular histogram) showing collective number of steps in any given direction (in 10-degree increments) in the presence of an HGF gradient.

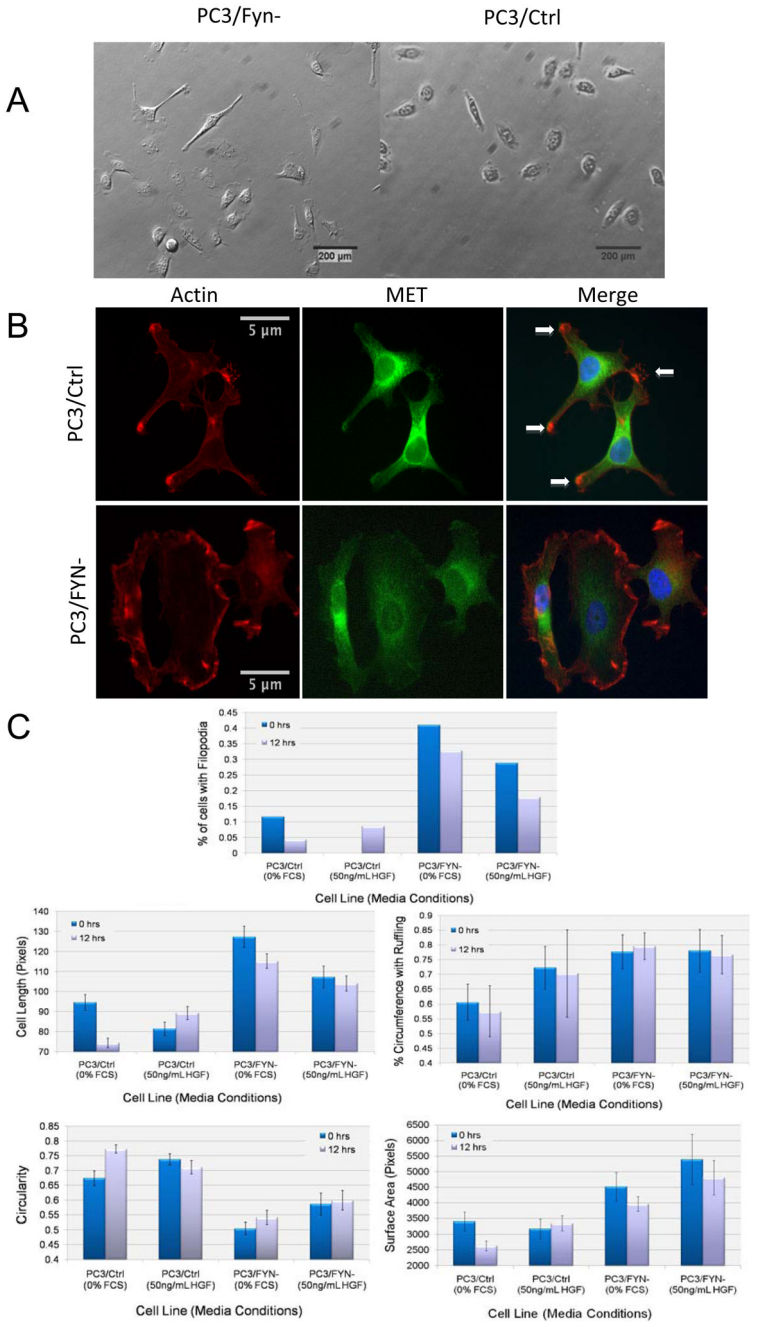

Figure 3.

A) Representative images of PC3/FYN- and PC3/Ctrl cells on polystyrene plates stimulated by HGF. PC3/FYN- cells were found to have greater cell length, area, and ruffling than PC3/Ctrl cells. B) Immunofluoresence of actin and MET in PC3 sublines. Overlap of actin and MET is shown in yellow and demarcated by arrows in the rightmost panels. These areas are most consistent with focal adhesion plaques. As seen in the lower right panel, there is no focal accumulation of both MET and actin to suggest plaque formation. B) Rose plots showing direction of movement of PC3 sublines relative to an HGF gradient (source on right). A rose plot is a circular histogram in 10 degree increments showing cumulative motion in any given direction in 360 degrees without regard to the magnitude of movement.

C) Graphical representation of quantified morphologic variations between PC3/FYN- and PC3/Ctrl cells.

A

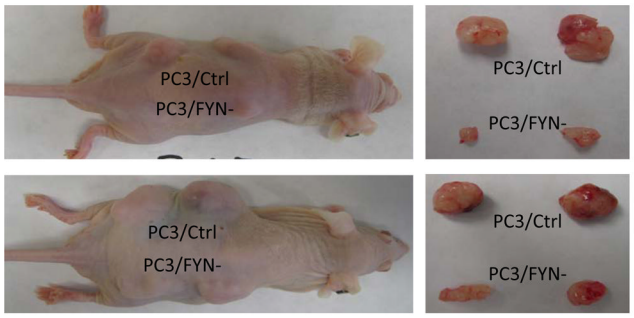

B

Mouse ID	Cross Product (mm2) PC3/Ctrl	PC3/FYN-	% change	Volume (mm3) PC3/Ctrl	PC3/FYN-	% change
3170	222	38	**17%**	1374	112	**8%**
3172	161	78	**49%**	878	350	**40%**
3173	196	95	**49%**	1236	443	**36%**
3174	314	181	**58%**	2347	1182	**50%**
3175	26	12	**48%**	63	20	**32%**

C

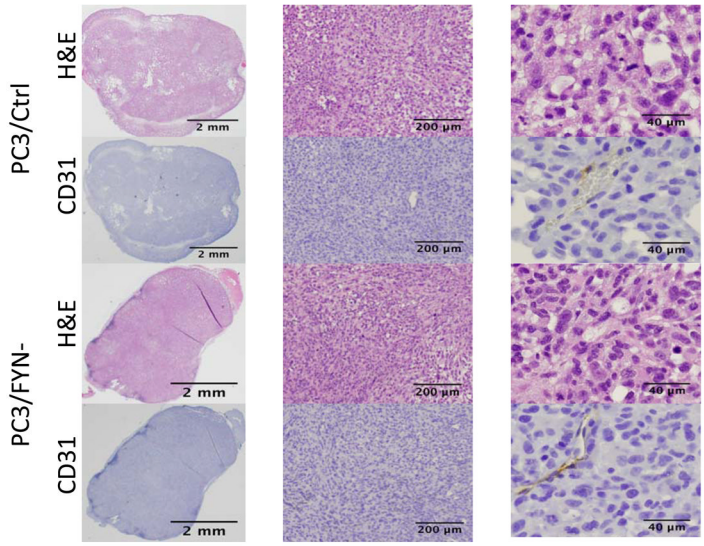

D

		Mitoses (per 10 HPF)	Tumor necrosis	Lymphoid aggregates (per 10 hpf)	Epithelioid-Spindled cells	Neovessels (# per 10 HPF)
PC3/FYN-	3170 R	42	<3%	<1	95:5	25
	3172 R	38	0%	0	90:10	32
	3174 R	46	2%	0	80:20	29
PC3/Ctrl	3170 L	56	10%	2	95:5	19
	3172 L	48	10%	1	90:10	25
	3174 L	51	6%	0	85:15	19

Figure 4.

A) (left panels)Nude mouse with subcutaneous injection of PC3/Ctrl and PC3/FYN- cells at day 57. (right panels) Tumor recovered at necropsy. B) Table of mouse tumor measurements showing both cross products (length x width) and volumetric approximations based on maximal and minimal tumor dimensions. C) Immuohistochemical analysis of tumors from *in vivo* growth study. PC3/Ctrl (top) and PC3/FYN- cells (bottom) were injected into the flanks of nu/nu mice and collected at necropsy. H&E and CD31 staining is shown at 1× (left panels), 4.2× (middle panels), and 20× (right panels). No significant change in cellular morphology or neovessel formation was seen between the two conditions. D) table of quantification of mitoses, tumor necrosis, lymphoid aggregate formation, ratio of epithliod to spindled cells, and neovessel density. No significant differences were seen.

Table 1

Summary of motility parameters from Dunn Chamber assay.

	PC3/FYN-	PC3/Ctrl	p value
Directionality	0.248	0.242	0.822
FMI	−0.042	0.084	0.077
AD	28.5 um	58.8 um	<0.001
ED	6.5 um	14.2 um	0.016
Velocity	0.16 μm/min	0.42 μm/min	<0.000001

FMI= forward motion index; AD= accumulated (total) distance; ED= Euclidean distance. Supplemental Figure 2 shows a graphical representation of the above parameters.

Table 2

Histomorphological analysis of tumors from *in vivo* growth assay (n=3 mice; no usable tissue was retrieved from the 4th mouse). Each row represents an analysis of 2 tumors (PC3/FYN- or PC3/Ctrl as indicated). Tumors were scored for number of mitoses, amount of necrosis (by volume), number of intratumoral lymphoid aggregates, amount of spindle morphology (i.e. high grade appearance), and neovessel formation (requiring both CD31 staining and luminal formation by pathologist's review).

		Mitoses (per 10 HPF)	Tumor necrosis	Lymphoid aggregates (per 10 hpf)	Epithelioid-Spindled cells	Neovessels (# per 10 HPF)
PC3/FYN-	**3170 R**	42	<3%	<1	95:5	25
	3172 R	38	0%	0	90:10	32
	3174 R	46	2%	0	80:20	29
PC3/Ctrl	**3170 L**	56	10%	2	95:5	19
	3172 L	48	10%	1	90:10	25
	3174 L	51	6%	0	85:15	19

Clin Cancer Res. Author manuscript; available in PMC 2012 May 15.